Journal of Medicinal Chemistry

Article

pubs.acs.org/jmc

Small Peptide Inhibitors of Acetyl-Peptide Hydrolase Having an Uncommon Mechanism of Inhibition and a Stable Bent Conformation

A. Sandomenico,[†] A. Russo,[†] G. Palmieri,[‡] P. Bergamo,[§] M. Gogliettino,[‡] L. Falcigno,[†,⊥] and M. Ruvo,*[,†]

[†]Istituto di Biostrutture e Bioimmagini, CNR, via Mezzocannone 16, 80134, Napoli, Italy

[‡]Istituto di Biochimica delle Proteine, CNR, via P. Castellino, 111, 80132, Napoli, Italy

[§]Istituto di Scienze degli Alimenti, CNR, via Roma 64, 83100, Avellino, Italy

[⊥]Dipartimento di Scienze Chimiche, Università di Napoli Federico II, via Cinthia, 80143, Napoli, Italy

Supporting Information

ABSTRACT: Acyl peptide hydrolase (APEH) catalyzes the removal of acetyl-amino acids from the N-terminus of peptides and cytoplasmic proteins. Due to the role played in several diseases, and to the growing interest around N-terminal acetylation, studies on APEH structure, function, and inhibition are attracting an ever increasing attention. We have therefore screened a random tetrapeptide library, N-capped with selected groups, and identified a trifluoroacetylated tetrapeptide (CF_3-lmph) which inhibits the enzyme with a K_i of 24.0 ± 0.8 μM. The inhibitor is selective for APEH, shows an uncommon uncompetitive mechanism of inhibition, and in solution adopts a stable bent conformation. CF_3-lmph efficiently crosses cell membranes, blocking the cytoplasmic activity of APEH; however, it triggers a mild pro-apoptotic effect as compared to other competitive and noncompetitive inhibitors. The unusual inhibition mechanism and the stable structure make the new compound a novel tool to investigate enzyme functions and a useful scaffold to develop more potent inhibitors.

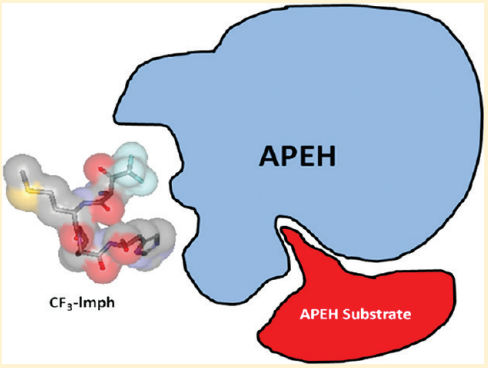

INTRODUCTION

Acyl peptide hydrolase (APEH) is a ubiquitous enzyme that belongs to the prolyl-oligopeptidase (POP) family of proteins. It mostly catalyzes the removal of *N*-acetyl-amino acids from the N-terminus of short peptides deriving from protein degradation processes and bearing residues with small hydrophobic side chains on position 1.[1] It has been also postulated for many years that it could be a key regulator of protein N-terminal acetylation; however, only very recently it has been shown that APEH can process a large set of full length cytoplasmic proteins, thus suggesting that their structure and function can be tightly regulated by the activity of this enzyme.[2] Indeed, treatment of cells with potent and highly specific APEH inhibitors leads to an accumulation of N-terminal acetylated proteins over the nonacetylated variants and to a sustained proliferation of mouse T cells, an effect not observed in untreated cells. Because a relevant fraction of cellular proteins is N-terminally acetylated[3] and this modification plays a critical role in the protein folding/misfolding process, thus on protein fate,[4] an obvious involvement of APEH in the protein turnover mechanism has been also hypothesized.[2,5]

We have recently demonstrated that APEH can influence the activity of proteasome,[6] a well-established target for a number of cancer diseases, including multiple myeloma.[7,8] APEH inhibitors have a potential as antitumor agents working as indirect regulators of the proteasome activity or more in general of the ubiquitin proteasome system (UPS).[5,9] In particular, we have reported that competitive inhibitors of APEH derived from the reactive site loop (RSL) of the first protein inhibitor of APEH isolated from the archaeon *Sulfolobus solfataricus*, SsCEI,[10] block the enzyme activity by a mechanism that leads to a concomitant downregulation of proteasome function, inducing a potent pro-apoptotic stimulus in human colon carcinoma cells (Caco-2). Remarkably, the same effects are seen using, alone or in combination with the peptide inhibitor, the $trans_{10}$-cis_{12} isomer of conjugated linoleic acid (CLA), which instead shows a noncompetitive mechanism of APEH inhibition. These findings open a new important perspective for the development of APEH inhibitors, especially in the field of multiple myeloma, an incurable tumor disease whose current treatments are mainly based on the use of proteasome inhibitors.[6] A further important role for APEH has been hypothesized in neurodegenerative diseases, such as Alzheimer's disease (AD), because administration of the acetylcholinesterase inhibitor dichlorvos to rat hippocampal slices also efficiently inhibits enzyme activity, and this correlates with improved synaptic efficacy.[11]

Received: October 7, 2011
Published: February 6, 2012

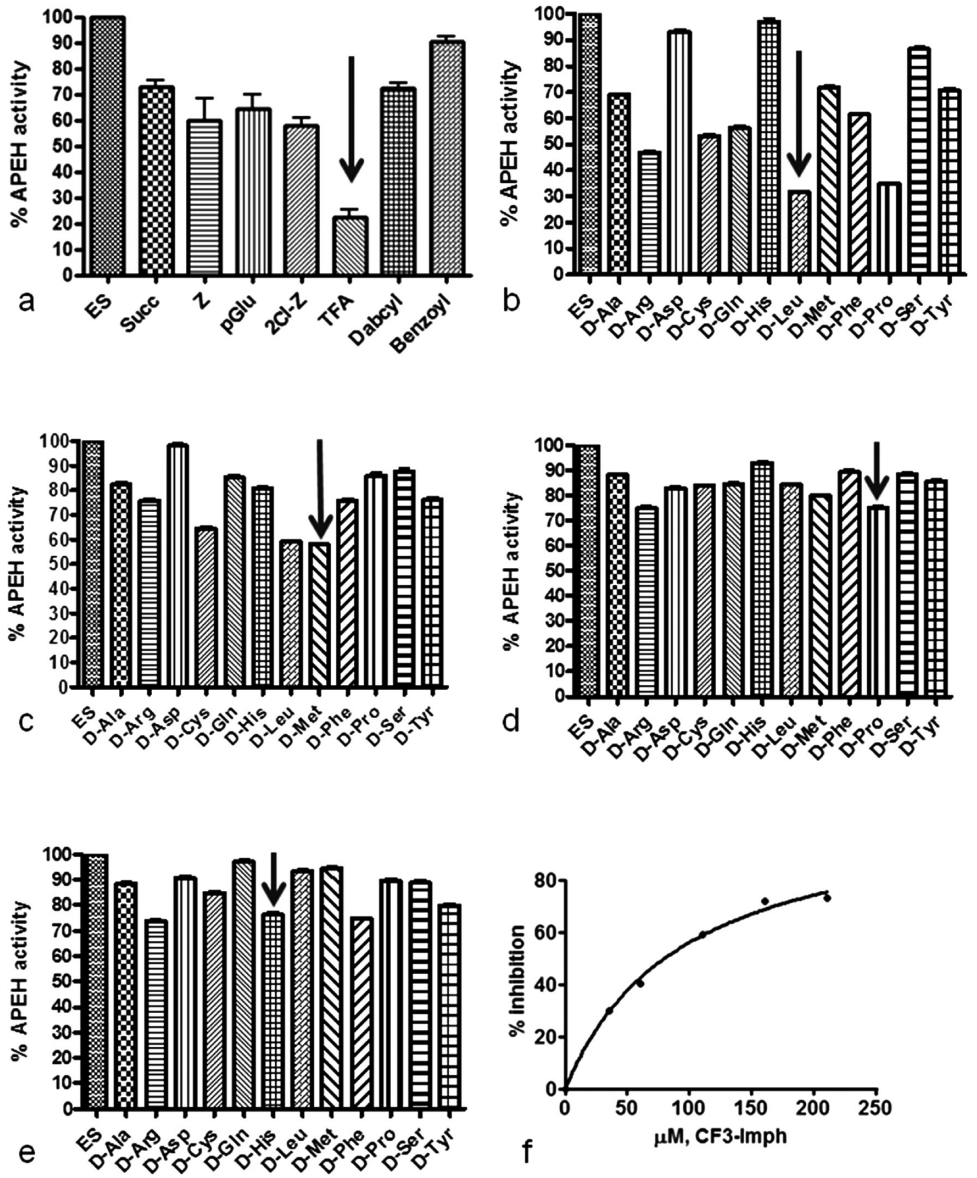

Figure 1. Iterative screening of the Yi-X1-X2-X3-X4 library to identify APEH inhibitors. The library was assembled in a simplified format (see Marasco et al.[12]) using a reduced set of residues accounting for all the different chemical groups present on natural amino acid side chains. D-Amino acids were used to obtain enzymatically stable peptides. Also the N-terminus was modified by a set of carboxylic acids in order to explore the chemical space around the N-terminus where APEH is known to operate. In part a, a plot with inhibition by the first sublibraries, distinguishable by the different carboxylic acids on the N-terminus, is reported. In part b, a plot with inhibition by the second set of sublibraries all N-terminally trifluoroacetylated, distinguishable by the different residues on position X1, is reported. In part c, a plot with inhibition by the third set of sublibraries, all having in common TFA-D-Leu, distinguishable by the different residues on position X2, is reported. In part d, a plot with inhibition by the fourth set of sublibraries, all having in common TFA-D-Leu-D-Met, distinguishable by the different residues on position X3, is reported. In part e, a plot with inhibition by the fifth set of sublibraries, all having in common TFA-D-Leu-D-Met-D-Pro, distinguishable by the different residues on position X4, is reported. In part f, the dose–response assay of TFA-D-Leu-D-Met-D-Pro-D-His to porcine liver APEH using acetyl-Ala-pNA as substrate is reported. The hyperbolic curve indicates the best fit for the percentage inhibition data obtained, and the IC_{50} value was calculated from the graph.

To further investigate the role played by APEH and their inhibitors on cell activity, we have undertaken the screening of a random library made of short synthetic peptides to select new compounds able to modulate the enzyme functions. Peptides are particularly suitable for this purpose for their capability to mimic the structures of natural substrates and of modulating enzyme activity by different mechanisms; in particular, small linear peptides could best fit in catalytic pockets and, given the high flexibility, they can adopt suitable conformations in an effective and timely way. Random screenings are very useful in this instance, as the protein structure is unknown and inhibitors cannot be designed on a rational basis. In addition, libraries of small peptides made of three to four residues and containing only subsets of amino acids are of particular interest for the rapid identification of small hits, which more favorably can be converted to more rigid and stable organic scaffolds.[12]

In this study, we have identified N-terminally modified small peptides (average MW 500–600 amu), selected from completely random synthetic libraries, which inhibit APEH in a very specific manner. The most active molecule also exhibits

dx.doi.org/10.1021/jm2013375 | J. Med. Chem. 2012, 55, 2102–2111

an uncommon mechanism of inhibition and a bent conformation induced by the presence of a D-proline on position 3. The peptide is not toxic compared to the commercially available APEH inhibitor ebelactone, efficiently crosses cell membranes, and blocks the activity of APEH in cancer cells. Although it exhibits only minor effects on cell proliferation and caspase 3 activity, its novel mechanism of action opens new perspectives for the understanding of the cellular processes involving APEH and the mechanisms associated to the parallel inhibition of proteasome activity.[6]

RESULTS

Library Preparation and Characterization. After the synthesis of the first library, an average 10 mg amount of material was obtained. Assuming an average MW of 600 amu and considering the synthesis scale of 20 μmoles, a rough 83% yield could be calculated. Data from amino acid analysis of peptide pools performed on the first (complexity 12^4 = 20 736 peptides) and second library (complexity 12^3 = 1728 peptides) were in agreement with a pretty equimolar distribution of peptide components within the mixtures. The third library (complexity 12^2 = 144 peptides) was not characterized. LC-MS analysis of 12-component mixtures also suggested that peptide components were essentially at the same concentration within mixtures. The synthesis of single peptides proceeded very smoothly. After HPLC purification, an average 50% yield was obtained. After semipreparative purification, tetrapeptides were all >95% pure, as determined by RP-HPLC as well as LC-MS analyses.

Library Screening. After the first screening step, the sublibrary trifluoroacetylated on the N-terminus was selected as the most active in inhibiting the APEH activity. It indeed provided an overall 78% enzyme inhibition at a concentration of 200 μM (see Figure 1a).

From the screening of the second library, tested at 40 μM, pools having D-Leu, D-Pro, and D-Arg on position X1 were selected as the most active. They provided inhibition of 67%, 64%, and 51%, respectively (Figure 1b). Testing of these sublibraries in a range of concentrations between 10 and 200 μM allowed the selection of the library with D-Leu as the most active (not shown). The 12 pools of the third library with TFA and D-Leu at the N-terminus were assayed at 100 μM. Pools with D-Cys(Acm), D-Met, and D-Leu were selected for the dose–response test and, as shown in Figure 1c, the library with D-Met on the X2 position was then selected for resynthesis. The 12 pools of the fourth library having the N-terminal common sequence TFA-D-Leu-D-Met were tested at 50 μM. In this assay, only pools with D-Pro and D-Arg on position X3 inhibited the enzyme (both 21%, Figure 1d). A dose–response test allowed selection of the pool with D-Pro as the candidate for resynthesis (not shown). The fifth library, composed of twelve single tetrapeptides, was tested at 50 μM. As reported in Figure 1e, peptides having D-Arg, or D-His, or D-Phe, or D-Tyr on position X4 were capable of inhibiting APEH for more than 25%; however, after testing in a dose–response assay, the peptide of sequence TFA-D-Leu-D-Met-D-Pro-D-His-NH_2 (hereafter termed only CF_3-lmph), was the one selected as an efficient inhibitor, as it was the only peptide able to block enzyme activity in a dose-dependent fashion. In Figure 2a the drawing structure of the selected tetrapeptide is reported, whereas in Figure 2b and 2c the structure of the inactive TFA-D-Leu-D-Met-D-Pro-D-Ala-NH_2 and TFA-D-Leu-D-Met-D-Pro-D-Asp-NH_2 (hereafter termed CF_3-lmpa and CF_3-lmpd, respectively), used as negative controls in the subsequent experiments, are reported.

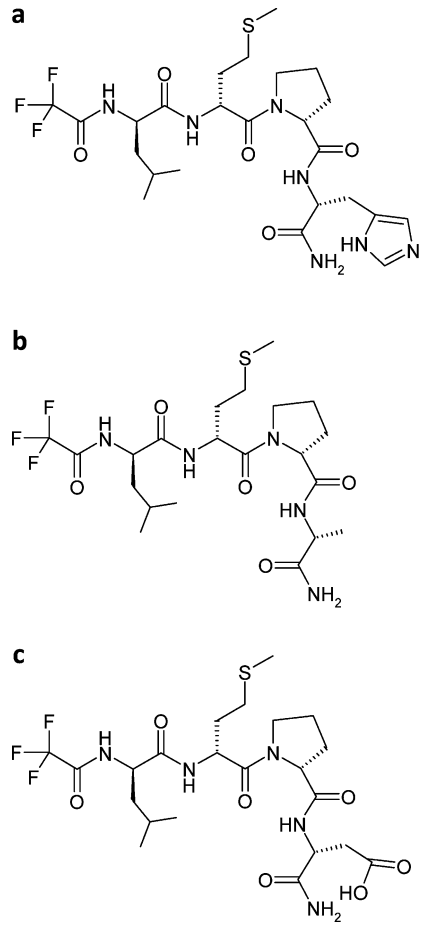

Figure 2. (a) Drawing structure of the selected active tetrapeptide TFA-D-Leu-D-Met-D-Pro-D-His-NH_2 (named CF_3-lmph). (b and c) The structures of the inactive variants TFA-D-Leu-D-Met-D-Pro-D-Ala-NH_2 and TFA-D-Leu-D-Met-D-Pro-D-Asp-NH_2 (termed CF_3-lmpa and CF_3-lmpd, respectively), used as negative control in the subsequent experiments, are shown.

Assessment of Peptide Selectivity and Mechanism of Inhibition. The inhibition activity of CF_3-lmph peptide was assessed using APEH purified from porcine liver, which shares more than 90% sequence identity with the homologous human enzyme. The selectivity of CF_3-lmph toward APEH was initially evaluated in biochemical assays using a panel of eukaryotic proteases (trypsin, α-chymotrypsin, elastase, carboxypeptidase Y, subtilisin, and proteinase K). Results (Table 3) show that the best protein target for CF_3-lmph was APEH with a maximum of 72% inhibition reached at 150 μM. This inhibition did not increase even using the peptide at 1 mM. The inhibition curve of porcine APEH followed a hyperbolic pattern with increasing inhibitor concentrations and gave an IC_{50} value of 98.0 ± 6.4 μM (Figure 1f). The affinity of CF_3-lmph toward porcine APEH was witnessed by a K_i value of 24.0 ± 0.8 μM. Data indicated that the peptide was also able to slightly affect carboxypeptidase activity (Table 3), reaching a maximum of 30% inhibition at 1.0 mM; the IC_{50} was only 210 ± 0.8 μM (see Figure SI 1 in Supporting Information). To determine the mechanism of APEH inhibition, we set out to use the peptide in several inhibition experiments, varying both substrate and peptide concentrations. Data are reported in Figure 3 as the

dx.doi.org/10.1021/jm2013375 | J. Med. Chem. 2012, 55, 2102–2111

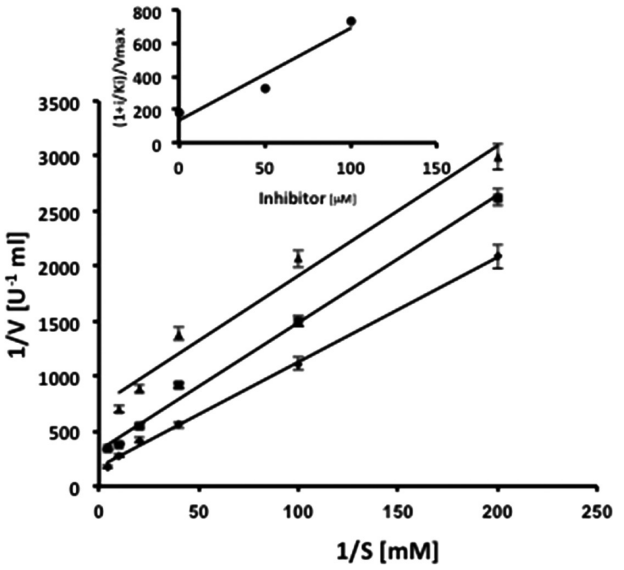

Figure 3. Double-reciprocal plots of the velocity against substrate (Ac-Ala-pNA) concentration at three different CF_3-lmph concentrations (no inhibitor ◆, 50 μM ■, and 100 μM ▲). The velocity of the reaction is expressed as μmol of *p*-nitroaniline released/min/mL on incubation at 37 °C. K_i value was determined from the equation of the uncompetitive inhibition (see insert for a plot of $[(1 + i/K_i)/V_{max}]$ vs inhibitor concentration).

classical Lineweaver–Burk double reciprocal plot, and the straight lines obtained at different inhibitor concentrations resulted in a series of parallel lines, which indicate that the tetrapeptide acts as a typical uncompetitive inhibitor. This very uncommon type of inhibition is based on a mechanism where the inhibitor binds to the enzyme, enhancing the binding of the substrate (so reducing K_m), but, due to a reduced reaction rate of the resultant enzyme–inhibitor–substrate complex, V_{max} is also decreased.[13]

Also the activity of the acetylated and nonacetylated variants was tested against porcine APEH to assess the role of the N-terminal trifluoroacetyl group. As reported in Figure 4, the

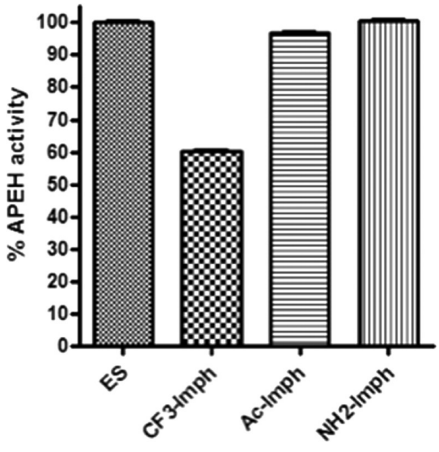

Figure 4. APEH inhibition by CF_3-lmph and the corresponding acetylated and NH_2-free peptides. Only the trifluoroacetylated peptide shows inhibition.

presence of this moiety confers a high specificity to peptide activity, because no enzyme inhibition was seen with the acetylated and the NH_2-free peptides.

Circular Dichroism. CF_3-lmph was characterized by CD and NMR spectroscopy in order to determine its conformational preferences and a possible correlation between its structure and the inhibition activity. For this purpose, CD spectra of the peptide at both pH 7.0 and pH 5.0 were acquired. In parallel also the CD spectrum of the N-terminally free variant was investigated under the same conditions. As can be seen in Figure 5, the peptide adopted a well-organized structure

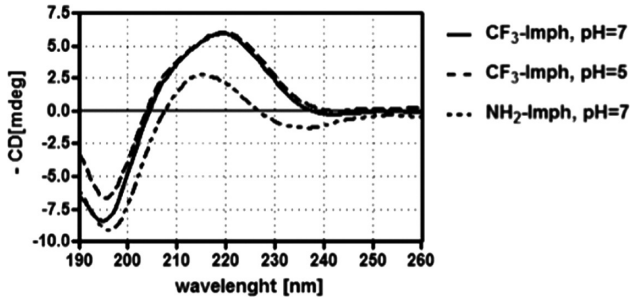

Figure 5. CD spectra of CF_3-lmph at pH 5.0 (solid line) and 7.0 (dashed line) at 200 μM. The spectrum of the NH_2-free peptide at pH 7.0 and at the same concentration (dotted line) is also reported. CD values at all wavelengths have been multiplied by −1 to take into account for the presence of all D residues.

with a minimum at 195 nm and a maximum at 220 nm. Considering the presence of all-D amino acids, which normally show inverted values, these spectra suggest that the peptide has a twisted or bent conformation at both pH values and that the structure is not grossly affected, at a qualitative level, by removing the trifluoroacetyl group.

NMR Spectroscopy. NMR investigation was performed on both the tetrapeptide inhibitor CF_3-lmph and on the inactive analogue CF_3-lmpa. The ala[4] variant, instead of that used as control in biochemical as well as cellular assays, was chosen because of its higher solubility at millimolar concentration.

NMR analyses in plain water showed that the two peptides CF_3-lmph and CF_3-lmpa adopt very similar conformations. Indeed, they showed comparable proton chemical shifts (Tables SI 1a, SI 1b of the Supporting Information), αCH chemical shifts deviations from random coil values[14] (Figure SI 2 of the Supporting Information) and NOE patterns. Interproton distances, evaluated from NOE intensities, were used in restrained molecular dynamics simulations to obtain solution molecular models of both peptides. Starting models were energy-minimized in a cubic box of water using Gromacs 4.0 program, as described in the Supporting Information. Before starting the dynamics simulations, the systems were further energy-minimized adding the NMR restraints, and the solvent was relaxed by a 200 ps MD at 300 K. Then, for each peptide, two simulations were run for 10 ns with (r) and without (u) NMR restraints to evaluate the stability of the peptide structure. The backbone root-mean-square deviations (rmsd) of both peptides along the trajectory at 300 K show small deviations (~1–1.5 Å) from the starting model, either for the restrained or for unrestrained molecular dynamics simulations, pointing to a stable structure over the observation time. The structural stability is well represented by the backbone superposition of molecular frames, collected during the last 2 ns of restrained MD simulations, of CF_3-lmph (rmsd 0.25 ± 0.10 Å) and CF_3-lmpa (rmsd of 0.34 ± 0.24 Å), and reported in Figure 6a and 6b. It should be noted that no

dx.doi.org/10.1021/jm2013375 | J. Med. Chem. 2012, 55, 2102–2111

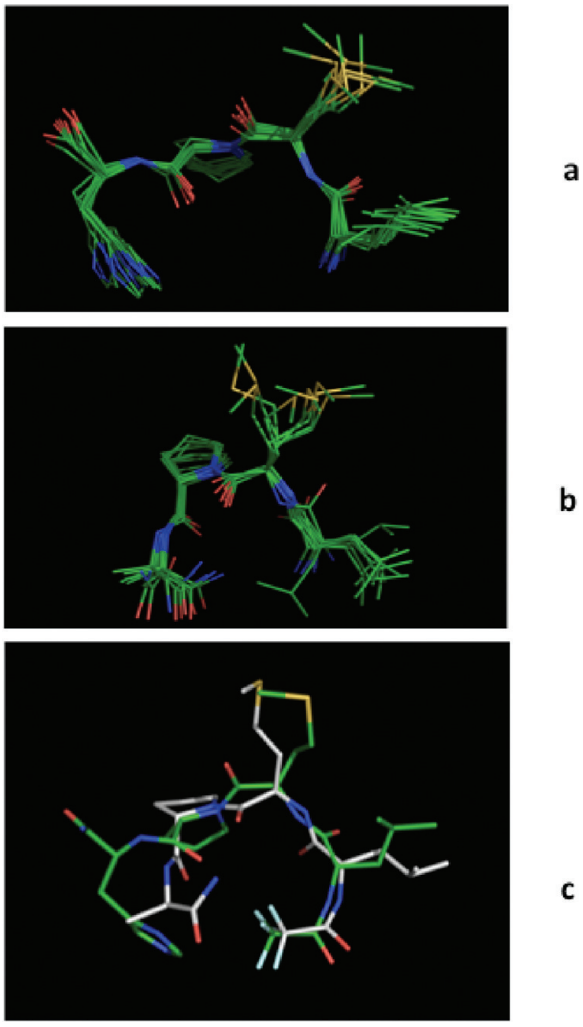

Figure 6. Backbone superposition of ten molecular frames collected during the last 2 ns of restrained molecular dynamics for (a) CF_3-lmph; (b) CF_3-lmpa. (c) Backbone superposition of CF_3-lmph (green) and CF_3-lmpa (gray) molecular models after 10 ns of restrained molecular dynamics.

structural differences were observed from restrained (r) and unrestrained (u) molecular dynamics simulations, and the comparison of the final r and u structures showed backbone rmsd of 0.34 Å and 0.20 Å for CF_3-lmph and CF_3-lmpa, respectively. The final molecular models obtained by restrained molecular dynamics simulations showed a good agreement with experimental NMR data and were chosen as representative of peptide structures. They look very similar in the conserved region (see Figure 6c) with a global backbone rmsd of 0.21 Å.

Cell Assays. The pro-apoptotic/cytotoxic effect produced by APEH inhibition was preliminarily investigated in HeLa cells exposed for 24 h to increasing concentrations of a widely used noncompetitive APEH inhibitor (i.e., ebelactone).[15] The marked (5-fold) increase of caspase 3 was produced by cell incubation with 30 and 50 μM ebelactone ($P < 0.001$) whereas its maximum cytotoxic effect (28%) was produced by cell exposure to 100 μM concentration. (Figure 7a).

Next, to determine the influence of CF_3-lmph or the control peptide TFA-D-Leu-D-Met-D-Pro-D-Asp-NH_2 (CF_3-lmpd) on cell viability, cell proliferation was evaluated upon exposure of HeLa cells for 24 h to increasing concentrations of the selected peptides. The dose-dependent antiproliferative effect was

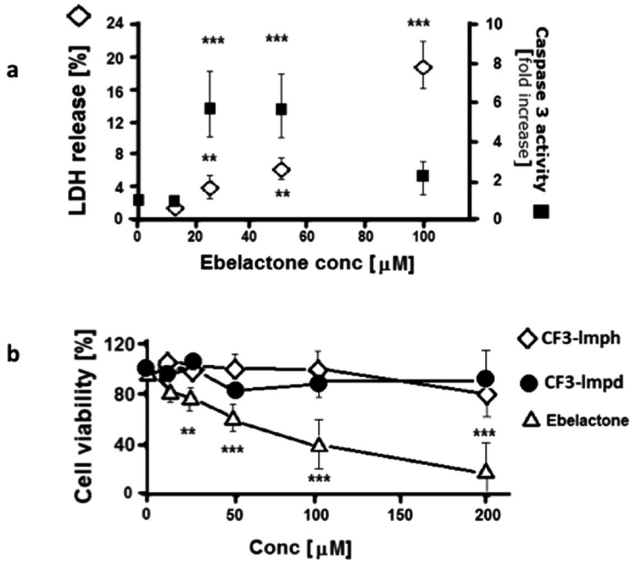

Figure 7. Pro-apoptotic and toxic effect of ebelactone on HeLa cells. The modulation of a commercially available APEH inhibitor on cell viability was preliminarily evaluated on HeLa cells. Caspase 3 activity and LDH release was evaluated upon 24 h exposure with increasing concentrations of ebelactone (a). Caspase 3 activity was expressed as fold increase as compared to untreated culture. Culture media from untreated culture were used as control, and those from cells exposed to 1% TritonX-100 were used as positive control (100% release). The dose-dependent effect of CF_3-lmph (open titled squares) or with the control peptide CF_3-lmpd (black circles) on cell viability was compared with that produced by ebelactone treatment (white triangles) (b). The data from triplicate analysis from three different experiments are expressed as means ± SD. ***, ** Significantly different $P < 0.005$ or 0.01, from respective controls.

produced by cell exposure to different ebelactone concentrations (positive control), but only minor changes were produced by the treatment with CF_3-lmph or CF_3-lmpd (Figure 7b).

In order to evaluate the ability of the peptide to inhibit APEH in in vitro experimental models, two cancer cell lines (A375 and HeLa) were exposed for 24 h with increasing concentrations of CF_3-lmph or of the control peptide CF_3-lmpd. As shown in Figure 8a and 8b, CF_3-lmph markedly reduced APEH activity in a dose-dependent manner, reaching their maximum effect at 150 μM, where enzyme activity was decreased in HeLa and in A375 cells by 80% and 50%, respectively. Notably, undetectable inhibition resulted from the treatment with CF_3-lmpd control peptide.

To determine the effects of CF_3-lmph or CF_3-lmpd on cell viability, their cytotoxic or pro-apoptotic effects were also studied. As apoptosis has been associated with APEH inhibition,[16] the caspase 3 activity, a key enzyme in the apoptotic cascade, was measured upon the cell treatments. Specifically, cells exposed to 100 or 150 μM CF_3-lmph, triggered a mild, but significant, increase in caspase 3 activity as compared with cells incubated with the same amount of control peptide ($P < 0.01$ or 0.005). In addition, undetectable toxicity, measured as LDH release in the medium, resulted from the CF_3-lmph-mediated inhibition of APEH (Figure 8c, 8d insert).

DISCUSSION AND CONCLUSIONS

APEH and other aminopeptidases are known to be essential for basic physiological processes, such as protein maturation[17] and

dx.doi.org/10.1021/jm2013375 | J. Med. Chem. 2012, 55, 2102–2111

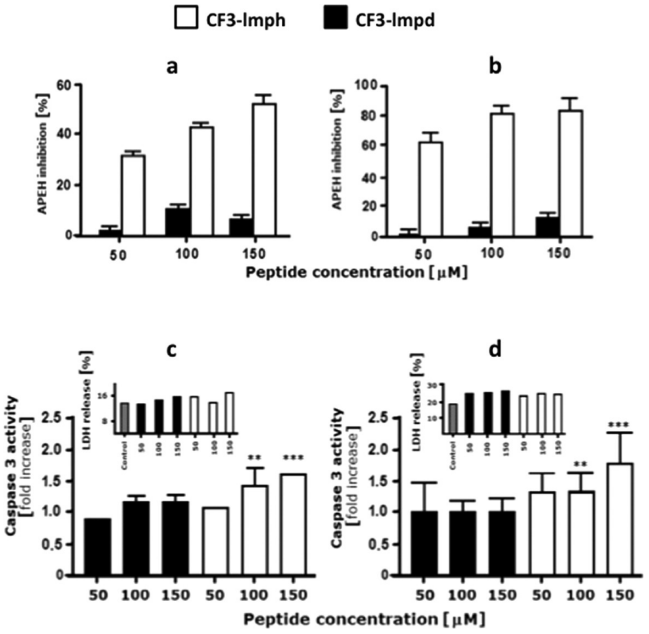

Figure 8. Down-regulation of APEH activity by CF_3-lmph in HeLa and A375 cells. APEH activity was measured in HeLa (a) or A375 (b) cells incubated with 50 μM, 100 μM and 150 μM CF_3-lmph (white bars) or with the control peptide CF_3-lmpd (black bars) for 24 h. Caspase-3 activities and LDH release were measured in HeLa (c) or A375 cells (d). The cytotoxic effect of the different treatments was evaluated by measuring the LDH release in the culture media. Media from untreated culture were used as control (gray bars). Media from cells exposed to 1% Triton X-100 were used as positive control (c, d insert). The data are expressed as means ± SD. ***, ** Significantly different $P < 0.005$ or 0.01, from respective controls.

cell cycle control.[18] Their inhibition disrupts protein turnover, leading to decreased cell survival and proliferation; thus, targeting this pathway has been indicated as a suitable approach for anticancer therapies.[19,20] Also a role in protein structure and function regulation has been persistently evoked for APEH due to its capability to remove acetyl-amino acids from the N-terminus of a large set of cytoplasmic proteins,[2] which, depending on the presence/absence of this small post-translational modification, could not properly fold and thus be tagged for degradation.[4,6] A more extensive understanding of APEH functions is thus needed, also in view of the recently reported involvement in the regulation of proteasome activity. This necessarily involves the development of specific modulators of enzymatic activity and a more detailed view of its interaction network and of related modulators. In this instance, enzyme inhibitors and interactors, with different mechanisms of action and structure, can play a major role, as they enable elucidation of downstream effects mediated by processed substrates or by interrupted or promoted interactions.

With the aim of developing new APEH inhibitors, we have prepared and screened a complex library of synthetic peptides modified on the N-terminus by a set of diverse chemical groups in order to investigate the space around the enzyme site of action and also to prevent undesired substrate-like behaviors of the peptides exposed to the enzyme. After five iterative rounds of screening and resynthesis needed to elucidate the whole peptide structure, we have identified the peptide CF_3-lmph as the one best inhibiting APEH in vitro. At variance with inhibitors previously described, the one we report in this study shows an uncommon uncompetitive mechanism of inhibition which is generally characterized by the binding of inhibitors to enzyme:substrate (ES) complexes and their inactivation induced by a delay in the release of processed substrates.

CF_3-lmph shows selectivity toward APEH, because, among the different serine proteases we have tested, it only blocks to a limited extent (30%) carboxypeptidase Y, with an IC_{50} which is more than twice that exhibited toward APEH (about 210 μM for carboxypeptidase Y and about 98 μM for APEH). The inhibition specificity is also demonstrated by the lack of activity of the acetylated and NH_2-free variants, indicating a direct involvement of fluorine atoms in the recognition and blocking of the ES complex. This is consistent with the observation that several organophosphorus compounds such as chlorpyrifos, dichlorvos, and naled, which share with the peptide the multihalogenated structure, also inhibit APEH.[21] We can thus reasonably hypothesize that halogens (bromine, fluorine, and chlorine), or more generally, highly electronegative centers, are likely an important discriminant for enzyme recognition.

Also the presence of D-histidine on position 4 of the tetrapeptide is very important for activity, and indeed mutants bearing D-Ala or D-Asp on the same position are not active. It is important to point out that the conformations of the inactive CF_3-lmpa and NH_2-lmph peptides are essentially identical to that of the active CF_3-lmph, with a bent conformation around the D-proline residue on position 3. This suggests that, beyond fluorines, the imidazole ring on the histidine side chain plays a crucial role in binding and inhibiting APEH. Again, given the strong structural similarity between imidazole and triazole rings, which are the core structures of many potent serine hydrolase inhibitors, we can reasonably speculate that the peptide shares with these at least one recognition site. Note that the peptide we have isolated in our screening does not apparently mimic any of the substrates recently identified for APEH,[2] still in agreement with the observation that CF_3-lmph does not bind into the catalytic pocket. Nevertheless, because potent triazole inhibitors have been isolated with competition assays, we can presume that the peptide inhibitor recognizes APEH on a region nearby the catalytic site.

While a role for APEH has been more clearly delineated in neurodegenerative diseases,[11] the occurrence of different phenotypic outcomes on cells treated with APEH inhibitors renders much more elusive the involvement of this enzyme in cancer.[9] The opposed effects observed certainly depend on the different experimental settings and cell lines utilized in the various studies; however, we cannot exclude that they could be associated to the mechanism of action of the diverse APEH inhibitors used, thus introducing a further level of complexity toward the understanding of the overall role played by this enzyme in cell homeostasis. We have recently reported that competitive APEH inhibition in Caco-2 cancer cells by SsCEI peptides reproducing the RSL of a proteic APEH inhibitor is paralleled by a downregulation of proteasome functions and an increase of caspase 3 activity that, in turn, induce a sustained and strong reduction of cell proliferation.[6] A similar effect is observed when the same cells are treated with the non-competitive inhibitor $trans_{10}$-cis_{12} CLA that binds the enzyme on a site adjacent to the catalytic pocket. Further, the effects are synergistic when the two compounds are used in combination.[6] On the contrary, the use of other competitive APEH inhibitors on mouse T cells strongly stimulates cell proliferation.[2]

To try to further address this very important aspect, we have used CF_3-lmph, along with an inactive control, to stimulate two

dx.doi.org/10.1021/jm2013375 | J. Med. Chem. 2012, 55, 2102−2111

different cell lines, A375 and HeLa, which are melanoma and cervical cancer cell lines, respectively. Though the peptide very efficiently crosses cell membranes, reduces enzyme activity in the cytoplasm, and is not toxic compared to other known inhibitors, for example ebelactone (see Figure 7a), it only slightly affects cell proliferation, inducing a reduction in cell vitality which is negligible compared to that of controls and to that previously observed in Caco-2 cells treated with competitive and noncompetitive inhibitors.[6] As also shown on mouse T cells, which even tend to proliferate when treated with APEH competitive inhibitors, this effect is certainly explained by the different cell lines used, which could display a different set of substrates, or by their metabolic status, but we cannot exclude that also the different mechanism of inhibition could influence cell proliferation by affecting or altering the network of interactions that regulates the functions of APEH. This hypothesis opens a new intriguing question regarding the role played by APEH nonsubstrate interactors, which are so far completely unknown.

We have identified the first uncompetitive APEH inhibitor, which is selective, has a conformationally defined structure, and contains molecular determinants common to other known inhibitors. In contrast to competitive inhibitors, which lose potency as substrate concentration rises, uncompetitive inhibitors become more potent as the substrate concentration increases in an inhibited open system.[22] This can be a significant advantage in vivo when the physiological context exposes the enzyme to high levels of substrate concentrations.

Despite the low potency in the micromolar range, the structural properties, the ease of synthesis, and unusual mechanism of action make this tetrapeptide an appealing and innovative tool for the systematic design of a new class of more potent and less toxic protease inhibitors, which may complement the active site-targeted molecules in future therapeutic applications.

EXPERIMENTAL SECTION

Materials. Protected amino acids for the synthesis of peptides were from GL-Biochem (Shanghai, PRC) and Novabiochem (Laufelfingen, Switzerland). Coupling agents were from GL-Biochem (Shanghai, PRC); solvents, such as acetonitrile (CH_3CN), dimethylformamide (DMF), and methanol (CH_3OH), were from Sigma-Aldrich (Milan, Italy). Chemicals for the preparation of libraries and enzymes for biochemical assays, including caspase-3 fluorimetric Assay Kits, and other chemicals of the highest purity were also from Sigma-Aldrich (Milan, Italy). Dulbecco's Modified Eagle Medium (DMEM), L-glutamine, penicillin–streptomycin, and fetal bovine serum (FBS) for cell culture were from Gibco-BRL. Porcine liver APEH was obtained by Takara. Acetyl-Ala-pNA was from Bachem.

Peptide Library Design, Synthesis, and Characterization. Peptide libraries were designed in a simplified format as reported in Marasco et al.[12] By this approach, a small set of amino acids is chosen to represent the chemical space occupied by very short peptides which can be seen as precursors or templates of small molecular scaffolds. Preferentially, only non natural or D-amino acids are included in these sets in order to potentially select enzyme-resistant new peptides. The set used here, reported in Table 1, includes aspartic acid as representative of amino acids with acidic side chains, arginine and histidine representing basic amino acids, glutamine and S-acetamidomethyl(Acm)-cysteine representing residues with amides on the side chain, phenylalanine and tyrosine as being representative of aromatic residues, serine representing residues with hydroxyl groups, leucine and methionine representing bulky hydrophobic amino acids, and alanine representing amino acids with small hydrophobic side chains. Proline was used to eventually select peptides with bent conformations. Note that histidine was used as an additional basic residue also by virtue of its aromaticity. The choice of this set of residues was also determined by their difference in MW in order to facilitate eventual identification of active components by tandem mass spectrometry methods.[12] As APEH is capable of removing acetyl-amino acids from the N-terminus of peptides and proteins, we set out to not acetylate the peptides but instead to introduce, on the N-terminal position, seven groups (see Table 2) with very different physicochemical properties in order to (i) prevent substrate-like effects and (ii) explore the chemical space around the N-terminal residue. These groups were chosen to introduce charges (succinic acid), aromatic groups (phenyl, Z, and 6-Cl-Z), bulky polyaromatic rings (Dabcyl), and small hydrophilic groups (trifluoroacetic acid (TFA) and pyroglutamate). The library was synthesized by the solid-phase

Table 1. Set of Amino Acids Used To Assemble the Tetrapeptide Library of General Formula Y_i-X_1-X_2-X_3-X_4-NH_2 on the X Position

N	building block, three-letter code	protected derivative used for the X positions
1	D-Ala	N^{α}-Fmoc-alanine
2	D-Arg	N^{α}-Fmoc-arginine (N^{Γ}-pentamethyldihydrobenzofuran)
3	D-Asp	N^{α}-Fmoc-aspartic acid (*tert*-butyl ester)
4	D-Cys(Acm)	N^{α}-Fmoc-cysteine(S-acetamydomethyl)
5	D-Gln	N^{α}-Fmoc-glutamine (N^{δ}-trityl)
6	D-His	N^{α}-Fmoc-histidine(N^{ε}-trityl)
7	D-Leu	N^{α}-Fmoc-leucine
8	D-Met	N^{α}-Fmoc-methionine
9	D-Phe	N^{α}-Fmoc-phenylalanine
10	D-Pro	N^{α}-Fmoc-proline
11	D-Ser	N^{α}-Fmoc- serine(*O*-*tert*-butyl-ether)
12	D-Tyr	N^{α}-Fmoc-tyrosine(*O*-*tert*-butyl-ether)

Table 2. Set of Carboxylic Acids Used To Modify the Tetrapeptide Library of General Formula Yi-X1-X2-X3-X4-NH_2 on the Yi Position

	Y_i	
N	building block	derivative used for modifying the N-terminus
1	Succ	succinic anhydride
2	Z	benzyloxycarbonyl-OSu
3	pGlu	pyroglutamic acid
4	2Cl-Z	2Cl-benzyloxycarbonyl-OSu
5	TFA	trifluoroacetic acid
6	Dabcyl	Dabcyl-OSu
7	benzoyl	benzoic acid

Table 3. Inhibition Profile of CF_3-lmph[a]

enzyme	pH	IC_{50} [μM]	maximal concentration tested [μM]	maximal inhibition [%]
APEH	7.5	98.0	1000	72
chymotrypsin	8.0*	>1000	1000	<1
elastase	8.0*	>1000	1000	<1
trypsin	8.0*	>1000	1000	<1
carboxypeptidase Y	7.0	210	1000	30
subtilisin	7.5	>1000	1000	<1
proteinase K	7.5	>1000	1000	<1

[a]The IC_{50} values of the tetrapeptide inhibitor were determined in 50 mM Tris-HCl (supplemented with 20 mM $CaCl_2$*) saline buffer at the optimal pH for the enzyme–substrate pair and at increasing concentrations, of CF_3-lmph, up to 1.0 mM.

dx.doi.org/10.1021/jm2013375 | J. Med. Chem. 2012, 55, 2102–2111

method on a global 140 μmol scale following the Fmoc/tBu methodology.[23] Fmoc deprotection was achieved by treatment with 30% piperidine in DMF. Couplings with amino acids or nonactivated carboxylic acids (3, 5, and 7 in Table 2) were performed by activating, with 1 equiv of HATU, 2 equiv of DIEA, and 10 equiv of Fmoc-protected amino acids or carboxylic acids. Random positions were obtained by coupling equimolar mixtures of the chosen set of amino acids used in very large excess to suppress preferential acylations deriving from differences in reactivity.

The first library was prepared by four sequential incorporations of mixtures of the 12 amino acids; the resin batch was then split into 7 identical aliquots to which the 7 different carboxylic acids were coupled. Subsequent libraries, identified by the iterative screening, were prepared in the same way and on the same synthesis scale. In the last step, 12 single peptides were prepared and purified before screening. Complex peptide mixtures were characterized by pool amino acid analysis comparing experimental amino acid distribution with those calculated assuming an equimolar distribution of all components in the pools. Single peptides and mixtures up to 12 components were easily characterized by LC-MS as reported elsewhere, identifying peptides by MW determination and in some cases by sequence assignment by tandem mass spectrometry. Cleavage of peptide mixtures from the resin was afforded by treatment with TFA−triisopropylsilane (TIS)−H_2O mixtures (90:5:5, v/v/v) and subsequent precipitation in cold diethyl ether. Single peptides were purified by semipreparative RP-HPLC on an ONYX 10 × 1 cm i.d. C18 monolithic column, operating at 15 mL/min, using H_2O and CH_3CN as eluents, both supplemented with 0.05% TFA. Gradients were chosen on the basis of peptide sequences. Libraries and single peptides were prepared as amidated derivatives. Canonical Fmoc-protected D-amino acids were used in all syntheses. D-Cys(Acm) was also introduced as the corresponding Fmoc derivative. A RINK amide resin with a 0.57 mmol/g substitution level was used in all syntheses. Most couplings and deprotection reactions were performed at room temperature for 5 min. In some specific cases, microwaves were used to improve reaction yields. A common kitchen microwave oven used at the minimum power was utilized for this purpose. Microwave-assisted couplings and deprotection reactions were carried out for 1.5 min with repeated 5 s on−off cycles. Cleavages were carried out in the same way for 1 min. After lyophilization, peptide material was dissolved in dimethyl sulfoxide (DMSO) at 10 mg/mL and stored frozen until use. Single peptides were characterized by RP-HPLC and LC-MS using an ONYX 50 × 2 mm i.d. C18 monolithic column, operating at 0.6 mL/min, using H_2O (eluent A) and CH_3CN (eluent B) as eluents, both supplemented with 0.05% TFA. Gradients were from 2% to 45% of eluent B in 9 min. Detection was achieved with a photodiode array set between 200 and 320 nm and with an ion trap mass spectrometer (Deca XP, ThermoFisher). Purity was checked on chromatograms extracted at 214 nm and on TIC (total ion current) traces obtained by full scans between 200 and 2000 m/z. Identity of peptides was confirmed by MW determination and tandem mass analyses. Peptides were all >95% pure, as determined by RP-HPLC and LC-MS analyses.

Enzyme Inhibition Assay and Screening of the Peptide Library. Porcine liver APEH activity was measured spectrophotometrically using the chromogenic substrate acetyl-Ala-pNA. The reaction mixture (0.2 mL) containing pure APEH (0.5 nM) in 50 mM Tris-HCl buffer, pH 7.5 (Tris buffer), was preincubated at 37 °C for 2 min. Then, 25 μM acetyl-Ala-pNA was added and the release of *p*-nitroanilide ($\varepsilon_{410\ nm}$ = 8800 M^{-1} cm^{-1}) was measured by recording the absorbance increase at 410 nm on a BIOTEK multiwavelength plate reader, equipped with a thermostatted compartment. APEH activity was expressed in IU. Assays were performed in 96-well polyethylene plates in duplicates or triplicates.

Inhibition by library components was carried out by using a fixed concentration of APEH (0.5 nM) and fixed concentrations of libraries as described below. Depending on the screening steps, peptide mixtures or single peptides were preincubated with the enzyme for 30 min at 37 °C before addition of the substrate, and the enzymatic activity was then followed as described above. Each inhibition experiment was carried out in duplicate wells. The first library (seven sublibraries) was screened in duplicate at a global concentration of 200 μM, assuming an average peptide molecular weight of 600 amu. Data were processed, averaging values from duplicate wells, and the slope was calculated by linear regression analysis. The percentage of inhibition was determined by comparing slopes from inhibition assays with that from the control experiment. To confirm and strengthen results after each screening step, dose−response assays with the positive mixtures were performed at concentrations ranging between 10 and 200 μM. In the second screening step, the 12 libraries bearing the trifluoroacetyl (TFA) group on the N-terminus were screened at a nominal concentration of 40 μM, assuming again an average MW of 600 amu. The same average molecular weight was assumed for the subsequent third (library concentration 100 μM) and fourth screening round (50 μM). Single peptides in the final fifth step were purified and characterized by LC-MS, assessing purity and identity. They were assayed at a concentration of 50 μM.

Enzyme Assays with APEH and Other Enzymes. Porcine liver APEH activity was measured spectrophotometrically using the chromogenic substrate acetyl-Ala-pNA. The reaction mixture (1 mL) containing pure APEH (38 ng) or an appropriate amount of cell extract in Tris buffer was preincubated at 37 °C for 2 min. Then, 25 μM acetyl-Ala-pNA was added and the release of *p*-nitroanilide (ε_{410} = 8800 M^{-1} cm^{-1}) was measured by recording the absorbance increase at 410 nm on a Cary 100 Scan (Varian) UV/vis spectrophotometer, equipped with a thermostatted cuvette compartment. APEH activity was expressed in IU. The carboxypeptidase Y, elastase, chymotrypsin-like activity of proteasome, trypsin, and subtilisin activities were evaluated according to previously published methods.[24] Proteinase K activity was measured according to the manufacturer's instructions.

Protease inhibiting activities of the selected peptides were carried out using a fixed amount of enzymes (5 nM) and increasing peptide concentrations, up to 1 mM. Mixtures were preincubated for 30 min at 37 °C before the addition of the substrate, and the enzymatic activities were followed as described above. To determine the mechanism of APEH inhibition, Lineweaver−Burk double reciprocal plots of data at increasing inhibitor and substrate concentrations were constructed. For this experiment, APEH (5 nM) was incubated, with or without inhibitor at 50 μM and 100 μM concentrations, and assayed at increasing substrate concentrations. The reciprocals of the rate of the substrate hydrolysis for each inhibitor concentration were plotted against the reciprocals of the substrate concentrations. The inhibition constant K_i was determined by the Lineweaver−Burk equation for the uncompetitive type of inhibition $[1/V = 1/V_{max} \times (1 + i/K_i) + (K_m/V_{max}) \times 1/S]$.

Circular Dichroism Analysis. CD spectra were obtained on a Jasco J-715 spectropolarimeter for peptide solutions at 2.0×10^{-4} M concentration in 5 mM Tris−HCl, pH 7.0, or in acetate buffer, pH 5.0, 25 °C. Hellma quartz cells of 1-cm path length were used in the far UV (190−250 nm). The temperature of the sample cell was regulated by a PTC-348 WI thermostat. Spectra were signal-averaged over three scans and baseline-corrected by subtracting a buffer spectrum. Due to the presence of only D residues, the entire spectrum was multiplied by −1.

NMR Analysis. NMR characterization of peptides was performed in water at 25 °C. Samples were prepared by dissolving weighted amounts of each peptide in water (spectroscopic purity), adding D_2O (ARMAR, isotopic purity 99,8%) for a final ratio 90/10 v/v. Final concentrations were ca. 2.0−2.5 mM. Details concerning NMR analyses are reported in the Supporting Information.

Molecular Dynamics (MD) Simulations. MD simulations were performed as reported in the Supporting Information.

Cell Cultures. Human melanoma (A375) and cervical cancer cells (HeLa), kindly donated by Dr. Rosanna Palumbo (IBB, CNR), were cultivated in DMEM supplemented with 10% FBS, 1 mM glutamine, and 100 units/mL penicillin−streptomycin at 37 °C in a humidified 5% CO_2 atmosphere. The cells were split using trypsin−ethylendiaminetetraacetic acid (EDTA) solution and plated in six-well plates at a density of 8×10^4 cells/mL, and the medium was replaced every 2−3 days. Cells at 60−70% confluence were incubated with the selected peptides at different concentrations.

Apoptosis Assays. The pro-apoptotic ability of the tetrapeptides were assayed by measuring the caspase-3 activity using fluorometric kits, according to the manufacturer instructions. These assays were based on hydrolysis of the substrate acetyl-Asp-Glu-Val-Asp-7-amido-4-methylcoumarin (Ac-DEVD-AMC) by caspase-3. The release of the 7-AMC moiety in protein extracts prepared from the differently treated cells was evaluated by fluorimetry (excitation 360 nm, emission 460 nm). Their amounts were calculated by means of a standard curve prepared with pure AMC, and following normalization for protein content, the activities were calculated as nmoles AMC/mg protein and expressed as fold increase as compared to control culture.

Cytotoxicity Assays. The release of LDH was used as the marker for cell toxicity.[25] The culture supernatants were sampled at the end of the incubations and centrifuged (4000*g*, 5 min, and 4 °C). Aliquots of the clear supernatant (10 μL) were incubated with 190 μL of reaction buffer (200 mM Tris/HCl, pH 8.0, 0.7 mM *p*-iodonitrotetrazolium violet, 50 mM L-lactic acid, 0.3 mM phenazine methoxysulfate, 0.4 mM NAD) for 30 min at 37 °C. Absorbance was measured at 490 nm, and the results were expressed as percentages of total LDH release from control cultures treated with 1% (w/v) Triton X-100 and calculated as:

$$[(\text{experimental value} - \text{blank value})/(\text{total lysis} - \text{blank value}) - 100]$$

Statistical Analysis. Data were obtained from triplicate analyses of three different preparations, and the results were expressed as means ± SD. Statistical analysis and IC_{50} values were calculated with the SigmaPlot 10.0 software through a nonlinear curve-fitting method and using a simple binding isotherm equation. Groups were compared by Student's *t* test, and $P < 0.05$ was considered as significant.

■ ASSOCIATED CONTENT

Ⓢ Supporting Information

Methods for NMR and MD simulations. A plot with dose–response carboxypeptidase Y inhibition. A plot with chemical shift deviations from random-coil values. This material is available free of charge via the Internet at http://pubs.acs.org.

■ AUTHOR INFORMATION

Corresponding Author

*Phone: 0039-081-2536644; fax: 0039-081-2534574; e-mail: menotti.ruvo@unina.it.

Notes

The authors declare no competing financial interest.

■ ACKNOWLEDGMENTS

The authors thank Dr. Giuseppe Perretta for his valuable assistance with peptide synthesis and Mr. Leopoldo Zona for kindly assisting during NMR experiments. The project has been partly funded by project FIRB MERIT N. RBNE08NKH7_003 (MIUR) to M.R. and by CNR.

■ ABBREVIATIONS USED

Acm, Acetamidomethyl; Caco-2, Human colon carcinoma cells; A375, Human melanoma cells; HeLa, Human cervical cancer cells; DMEM, Dulbecco's Modified Eagle Medium; DMSO, Dimethylsulfoxide; EDTA, Ethylendiamine-tetra-acetic acid; FBS, Fetal Bovine Serum; TFA, Trifluoroacetic acid; TIS, Tri-isopropylsilane

■ REFERENCES

(1) Perrier, J.; Durand, A.; Giardina, T.; Puigserver, A. Catabolism of intracellular N-terminal acetylated proteins: involvement of acylpeptide hydrolase and acylase. *Biochimie* **2005**, *87*, 673–685.

(2) Adibekian, A.; Martin, B. R.; Wang, C.; Hsu, K. L.; Bachovchin, D. A.; Niessen, S.; Hoover, H.; Cravatt, B. F. Click-generated triazole ureas as ultrapotent in vivo-active serine hydrolase inhibitors. *Nat. Chem. Biol.* **2011**, *7*, 469–478.

(3) Narita, K. Isolation of acetylpeptide from enzymic digests of TMV-protein. *Biochim. Biophys. Acta* **1958**, *28*, 184–191.

(4) Forte, G. M.; Pool, M. R.; Stirling, C. J. N-terminal acetylation inhibits protein targeting to the endoplasmic reticulum. *PLoS Biol.* **2011**, *9*, e1001073.

(5) Shimizu, K.; Kiuchi, Y.; Ando, K.; Hayakawa, M.; Kikugawa, K. Coordination of oxidized protein hydrolase and the proteasome in the clearance of cytotoxic denatured proteins. *Biochem. Biophys. Res. Commun.* **2004**, *324*, 140–146.

(6) Palmieri, G.; Bergamo, P.; Luini, A.; Ruvo, M.; Gogliettino, M.; Langella, E.; Saviano, M.; Hegde, R.; Sandomenico, A.; Rossi, M. Acyl Peptide hydrolase Inhibition as targeted strategy to induce proteasomal dysfunction. *PLoS One* **2011**, *6* (10), e25888.

(7) Orlowski, R. Z.; Kuhn, D. J. Proteasome inhibitors in cancer therapy: lessons from the first decade. *Clin. Cancer Res.* **2008**, *14*, 1649–1657.

(8) Landis-Piwowar, K. R.; Milacic, V.; Chen, D.; Yang, H.; Zhao, Y.; Chan, T. H.; Yan, B.; Dou, Q. P. The proteasome as a potential target for novel anticancer drugs and chemosensitizers. *Drug Resist. Updates* **2006**, *9*, 263–273.

(9) Scaloni, A.; Jones, W.; Pospischil, M.; Sassa, S.; Schneewind, O.; Popowicz, A. M.; Bossa, F.; Graziano, S. L.; Manning, J. M. Deficiency of acylpeptide hydrolase in small-cell lung carcinoma cell lines. *J. Lab. Clin. Med.* **1992**, *120*, 546–552.

(10) Palmieri, G.; Langella, E.; Gogliettino, M.; Saviano, M.; Pocsfalvi, G.; Rossi, M. A novel class of protease targets of phosphatidylethanolamine-binding proteins (PEBP): a study of the acylpeptide hydrolase and the PEBP inhibitor from the archaeon Sulfolobus solfataricus. *Mol. Biosyst.* **2010**, *6*, 2498–2507.

(11) Olmos, C.; Sandoval, R.; Rozas, C.; Navarro, S.; Wyneken, U.; Zeise, M.; Morales, B.; Pancetti, F. Effect of short-term exposure to dichlorvos on synaptic plasticity of rat hippocampal slices: involvement of acylpeptide hydrolase and alpha(7) nicotinic receptors. *Toxicol. Appl. Pharmacol.* **2009**, *238*, 37–46.

(12) Marasco, D.; Perretta, G.; Sabatella, M.; Ruvo, M. Past and future perspectives of synthetic peptide libraries. *Curr. Protein Pept. Sci.* **2008**, *9*, 447–467.

(13) Segel, I. H. Enzyme kinetics; Wiley Interscience: New York, 1975; pp 161–166.

(14) Wishart, D. S.; Sykes, B. D.; Richards, F. M. Relationship between nuclear magnetic resonance chemical shift and protein secondary structure. *J. Mol. Biol.* **1991**, *222*, 311–333.

(15) Abe, F.; Aoyagi, T. Physiological roles of ectoenzymes indicated by the use of aminopeptidase inhibitors. In *Ectopeptidases. CD13/Aminopeptidase N and CD26/Dipeptidylpeptidase IV in Medicine and Biology*; Langner, J., Ansorge, S., Eds.; 2002.

(16) Yamaguchi, M.; Kambayashi, D.; Toda, J.; Sano, T.; Toyoshima, S.; Hojo, H. Acetylleucine chloromethyl ketone, an inhibitor of acylpeptide hydrolase, induces apoptosis of U937 cells. *Biochem. Biophys. Res. Commun.* **1999**, *263*, 139–142.

(17) Moerschell, R. P.; Hosokawa, Y.; Tsunasawa, S.; Sherman, F. The specificities of yeast methionine aminopeptidase and acetylation of amino-terminal methionine in vivo. Processing of altered iso-1-cytochromes c created by oligonucleotide transformation. *J. Biol. Chem.* **1990**, *265*, 19638–19643.

(18) Constam, D. B.; Tobler, A. R.; Rensing-Ehl, A.; Kemler, I.; Hersh, L. B.; Fontana, A. Puromycin-sensitive aminopeptidase. Sequence analysis, expression, and functional characterization. *J. Biol. Chem.* **1995**, *270*, 26931–26939.

(19) Wickstrom, M.; Larsson, R.; Nygren, P.; Gullbo, J. Amino-peptidase N (CD13) as a target for cancer chemotherapy. *Cancer Sci.* **2011**, *102*, 501–508.

(20) Moore, H. E.; Davenport, E. L.; Smith, E. M.; Muralikrishnan, S.; Dunlop, A. S.; Walker, B. A.; Krige, D.; Drummond, A. H.; Hooftman, L.; Morgan, G. J.; Davies, F. E. Aminopeptidase inhibition

as a targeted treatment strategy in myeloma. *Mol. Cancer Ther.* **2009**, *8*, 762−770.
(21) Casida, J. E.; Quistad, G. B. Serine hydrolase targets of organophosphorus toxicants. *Chem. Biol. Interact.* **2005**, *157−158*, 277−283.
(22) Westley, A. M.; Westley, J. Enzyme inhibition in open systems. Superiority of uncompetitive agents. *J. Biol. Chem.* **1996**, *271*, 5347−52.
(23) Fields, G. B.; Noble, R. L. Solid phase peptide synthesis utilizing 9-fluorenylmethoxycarbonyl amino acids. *Int. J. Pept. Protein Res.* **1990**, *35*, 161−214.
(24) Palmieri, G.; Catara, G.; Saviano, M.; Langella, E.; Gogliettino, M.; Rossi, M. First Archaeal PEPB-Serine Protease Inhibitor from Sulfolobus solfataricus with Noncanonical Amino Acid Sequence in the Reactive-Site Loop. *J. Proteome Res.* **2009**, *8*, 327−334.
(25) Decker, T.; Lohmann-Matthes, M. L. A quick and simple method for the quantitation of lactate dehydrogenase release in measurements of cellular cytotoxicity and tumor necrosis factor (TNF) activity. *J. Immunol. Methods* **1988**, *115*, 61−69.